E. W. Smith and K. J. Pascoe†*

Biaxial Fatigue of a Glass-Fibre Reinforced Composite. Part 1: Fatigue and Fracture Behaviour

REFERENCE Smith, E. W. and Pascoe, K. J., **Biaxial fatigue of a glass-fibre reinforced composite. Part 1: fatigue and fracture behaviour**, *Biaxial and Multiaxial Fatigue*, EGF 3 (Edited by M. W. Brown and K. J. Miller), 1989, Mechanical Engineering Publications, London, pp. 367–396.

ABSTRACT The biaxial monotonic and fatigue strength properties of a woven roving glass reinforced polyester composite have been established using flat cruciform-shaped specimens. Five biaxial stress states were tested with the warp fibres at various angles to the major principal stress.

Failure was caused solely by rectilinear cracking and delamination when the in-plane principal stresses were aligned with the fibres. In contrast, for pure in-plane shear loading with the fibre weave aligned along the shear plane, no signs of macrocracking were apparent and failure was due to fibre/matrix interface shear degradation. The general off-axis loading case showed both modes of failure.

Introduction

During the past 25–30 years the development of fibre reinforced composite materials has led to their use in many advanced structures due to their inherent high strength, low weight, specific electrical, acoustic, and magnetic properties, and their ability to be tailored to meet complex shape and strength problems. Unfortunately the special properties and especially the high strength which may be afforded by fibre reinforcement are accompanied by marked strength anisotropy (1)–(3), particularly if the fibres are of unidirectional array or aligned along specific axes. Thus, when designing a structure, the great versatility of composites is somewhat nullified as the principal stress *directions* as well as the principal stress levels become of paramount importance. Also it must be remembered that the states of stress so often referred to as 'simple' tension, compression, bending, or torsion are seldom encountered in practical engineering applications.

Composite materials, like most engineering materials, can fail by fatigue (4)–(5). The mechanisms of cyclic dependent failure are not wholly understood in conventional materials, but the fatigue process in composites is further complicated by the presence of the fibre/matrix interface (6)–(8). The importance of the interface is such that fibre composites are often thought of as three-phase materials: fibre, matrix, and interface. The fibres carry load and so

* Department of Production Technology, Massey University, Palmerston North, New Zealand.
† University Engineering Department, Cambridge, UK.

give strength, the matrix is there to redistribute stress, and the interface transmits stress between fibre and matrix, and, of the three, the last is characteristically the weakest link. The fatigue process in metallic materials consists of crack initiation, propagation, and final failure and though a number of cracks may initiate and propagate, it is only one crack which propagates to cause fracture (**9**). In fibre-reinforced composites fatigue also consists of crack initiation, propagation, and final failure, but final failure is caused by the accumulation and propagation of many cracks; it is a bulk process (**10**). Fatigue damage is apparent from losses in both modulus and strength (**11**)–(**12**).

The purpose of this paper is to describe the behaviour of a woven roving glass-fibre polyester composite subjected to monotonic and cyclic in-plane biaxial loading. The findings were obtained from tests on flat cruciform-shaped specimens subjected to five different states of in-plane biaxial stress and with the fibres orientated at angles of 0, $22\frac{1}{2}$, and 45 degrees to the principal stress directions. This work, chronologically, is a continuation of the research of Pascoe and de Villiers (**13**) and Parsons and Pascoe (**14**), who looked at the fatigue behaviour of steels under biaxial cyclic stress.

Notation

m', c	Material constants
mcr	Minimum creep rate
N_f	Fatigue life
t_r	Creep rupture life
$\dot{\varepsilon}_{min}$	Minimum strain range accumulation rate
λ	Load ratio (σ_x/σ_y)
σ	Maximum principal stress
σ_x, σ_y	Applied and principal stresses

Review of tests on glass-reinforced plastics under biaxial stress

Experimental methods for obtaining a 'biaxial' state of stress in metals are numerous (see, for example, review of Evans (**15**)). The most versatile and much used method is the tubular specimen subject to any combination of axial tension/compression, torsion (**16**), or internal/external pressure (**17**), to give an infinite number of states of complex stress. Flat cruciform-shaped specimens, though not so versatile in respect of the through-thickness stress state, have also been used with success (**13**)(**18**). However, the application of these techniques to the biaxial testing of glass-reinforced plastic has been limited. Isolated instances of biaxial compression (**19**) and biaxial flexure (**20**) may be cited, but details are scant. The adoption of a cruciform-shaped specimen to assess the effects of complex stress on reinforced plastics has been attempted by Bert *et al.* (**21**), who carried out static tensile tests on woven-cloth-reinforced epoxy laminates under biaxial load ratios of 1 : 2, 1 : 1, and 2 : 1. No negative load ratios were tested using cruciform specimens and tubular specimens were used to obtain shear strength data. They concluded that the stress/strain limit of

proportionality was higher under biaxial loading than uniaxial, but the apparent biaxial ultimate strengths were generally less than the uniaxial values.

Owen and Found (**22**) studied the effects of biaxial monotonic and fatigue loading on chopped-strand-mat/polyester composites using thin-walled tubes subject to combinations of axial load and internal pressure which gave principal stress ratios of 1, $+\frac{1}{2}$, 0, $-\frac{1}{2}$, and -1. All tests were load controlled. In-plane shear strengths were obtained from four-point bend tests using specimens with a span/depth ratio of 3. The equi-biaxial (tension–tension) loading case caused rapid development of fibre debonding and resin cracking and was seen to be the most damaging load ratio. Owen and Griffiths (**23**) and Owen and Rice (**24**) extended this work to the testing of fabric-reinforced polyester composites. Limited experimental biaxial fracture data have also been collected from tests on tubular specimens (**25**)–(**26**).

Experimental background

The biaxial hydraulic servo-controlled rig developed at the Cambridge University Engineering Department (**27**) was used for all the tests. This machine will test biaxial cruciform specimens for any phase of principal in-plane loadings up to ±200 kN. Nine biaxial and three uniaxial stress states were tested as outlined in Fig. 1.

One batch of test material was used for the whole programme. The laminate was laid up from reinforcement of glass-fibre woven roving, Marglass 266 24 oz (Fothergill and Harvey Ltd), and an isophthalic polyester resin, BP 2785 CV (BP Chemicals). The warp and weft fibres were balanced and the rovings had a weave of 5 mm width. Lamina thickness as laid up averaged 0.9 mm and the test laminate contained 13 laminae. The nominal resin content was 46 per cent. The weft fibres are designated as the 0 degree weave direction.

A biaxial specimen and a 50 mm wide parallel-sided uniaxial specimen are shown in Fig. 2. The biaxial cruciform specimens were 300 mm × 300 mm and of 12 mm nominal thickness with a 60 mm square flat working section. Grip reinforcement with duralumin plate was necessary to avoid fracture in the arms; the specimens were bolted to the four loading arms.

Measurement and monitoring of the specimen strain throughout the fatigue test life proved difficult due to the material's heterogeneous nature, low modulus and gradual break-up of the specimen surface as damage progressed. Surface bonded strain gauges even for monotonic loading were found to give poor results and conventional uniaxial extensometers were found unsatisfactory due to their geometry and method of attachment. Hence special extensometers based on bending of a short resistance-strain-gauged double cantilever beam (**28**) were developed. Either load cell or strain extensometer signals could be used for the servo control. Preliminary work showed that strain control of fatigue tests on grp would tend to give an increased life over the equivalent load controlled test: this is borne out by the work of Agarwal and Dally (**12**). All tests reported herein were under load control. The load ratio, λ,

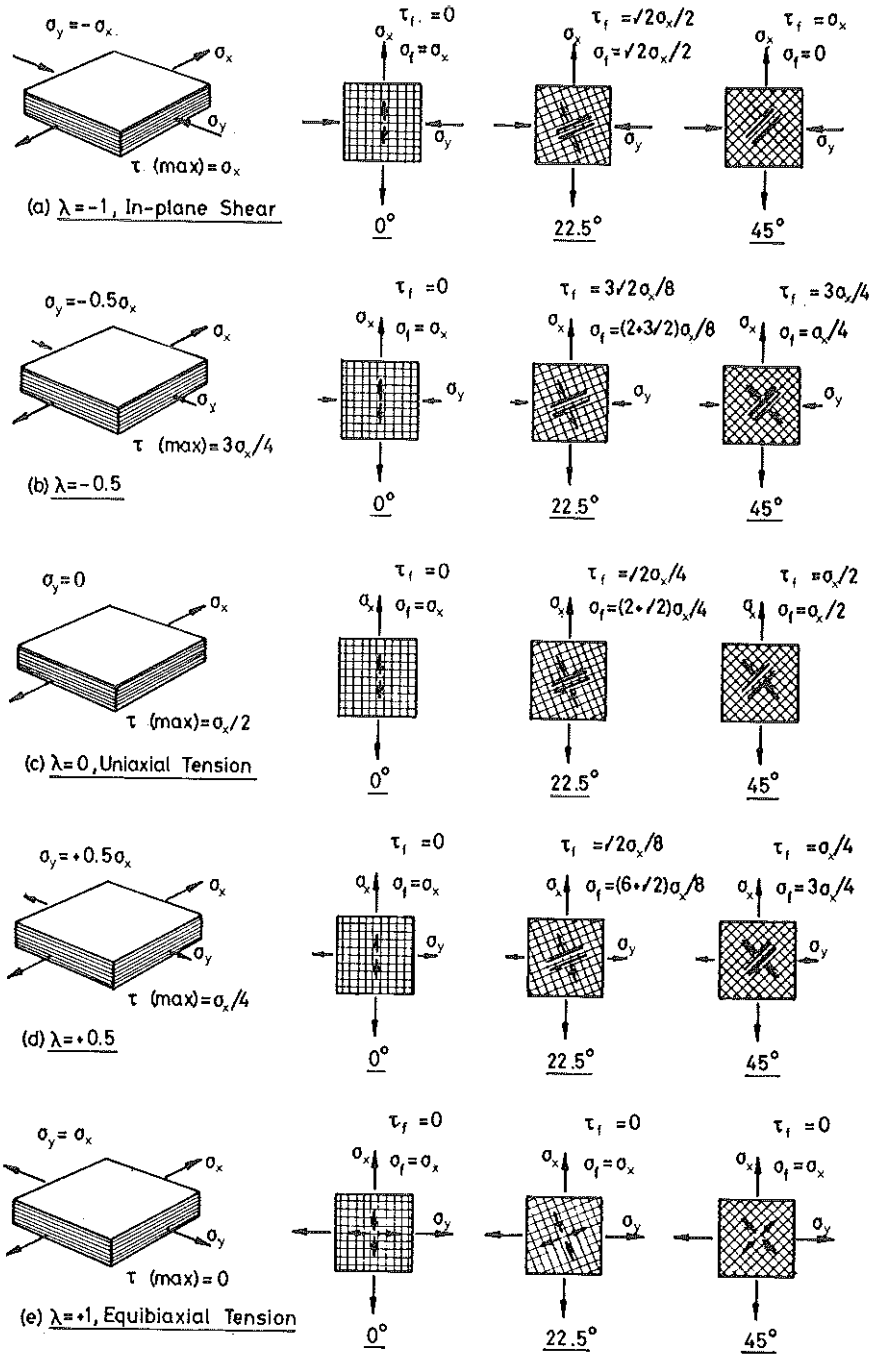

Fig 1 Biaxial stress states, showing the normal and shear stress components aligned with the fibre direction. σ_f is maximum component of tensile stress normal to fibre τ_{12}. τ_{12} is shear stress component along fibre

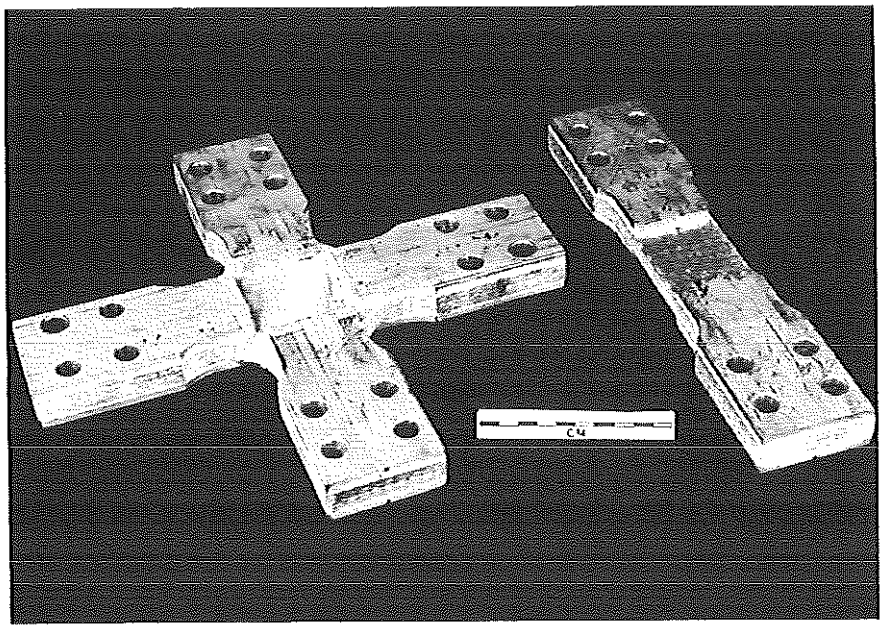

Fig 2 Biaxial and uniaxial grp test specimens

is defined as the ratio of the maximum (or tensile) to minimum (or compressive) principal load; all tests were for zero mean loads. Fatigue test frequencies were generally kept in the range 0.1–0.6 Hz to prevent excessive cyclic induced heating.

Various techniques have been proposed to quantify progressive fatigue damage.

(a) Observation of cracking density at a free edge or at a through-thickness section of a specimen (**10**).
(b) Measurement of decrease in apparent modulus (**11**)(**12**)(**29**).
(c) Assessment of specimen opacity by light transmission (**30**)(**31**).
(d) Measurement of water absorption (**32**).
(e) Measurement of acoustic emissions (**33**).

Attempts were made to measure crack density and specimen opacity, but the most reliable and effective technique for monitoring progressive damage was found to be by observation of the progressive stress/strain loops; much of the discussion in this paper will be centred on their shape and nature.

Uniaxial and biaxial monotonic failure

Uniaxial monotonic loading ($\lambda = 0$)

Though the uniaxial monotonic stress/strain behaviour of many types of glass-fibre reinforced plastics has been documented by a number of researchers,

e.g., (34)(35), it was necessary to carry out some uniaxial monotonic tests for a better understanding of the biaxial stress/strain behaviour. The uniaxial stress/strain curves for the test grp are shown in Fig. 3 for loading in tension and compression in various directions. Nominal strain rates were $10^{-3}\,s^{-1}$.

Under tensile loading along the fibre axes a distinct 'knee' is observed with the stress/strain curve showing linearity both above and below this 'knee'. It is due to a combination of two related damage phenomena.

(1) Breakdown of the glass/resin bond in the rovings running transverse to the principal stress direction.
(2) Cracking within the resin-rich areas; cracks running perpendicular to the principal stress.

The knee occurs at almost the same stress level for both weft (0 degrees) and warp (90 degrees) direction.

In the weft (0 degrees) direction, apart from the knee, stress/strain linearity occurs up to approximately 90 per cent of the ultimate stress and above this level delamination causes a progressive drop in modulus whereas in the warp (90 degrees) direction the modulus above the knee falls away at a much lower stress level (145 MPa or 55 per cent ultimate). The weft fibres lie relatively straight and as a consequence the warp fibres must weave above and below them; the progressive non-linearity in the weft direction is the result of straightening of these fibres. At approximately 90 per cent ultimate stress the modulus is further reduced by delamination.

The initial moduli, strengths, and failure strains are all greater in the warp (90 degrees) direction than the weft (0 degrees) direction. This was not expected as the roving reinforcement is balanced, i.e., the number of fibres per roving in the warp and weft are the same. However, it was noticed that the width of the warp (90 degrees) rovings was less than that of the weft (0 degrees) rovings, i.e., as laid up the laminate contained more warp rovings than weft rovings per unit width.

As well as causing a drop in modulus, resin cracking and fibre debonding also stop cross-coupling between longitudinal and transverse strains. Poisson's ratio is constant in both warp and weft directions up to the 'knee', but above the 'knee' the transverse strain no longer increases and at approximately 70 per cent ultimate stress shows a decrease. Prior to failure the Poisson's ratio may be of the order of 0.05 or less.

For both axes final failure is preceded by excessive delamination. Delamination at these high stress levels is seen to be a 'stop–start' process with the area of cross-over of adjacent rovings suddenly parting or delaminating from its neighbour, then as the load increases a further area delaminates. There was no sign of early fibre failure and, apparently, once fibres did fail, then final failure followed without control.

In contrast, under compressive loading there are no signs of fibre debonding or resin cracking and delamination is visible only just prior to final failure. This

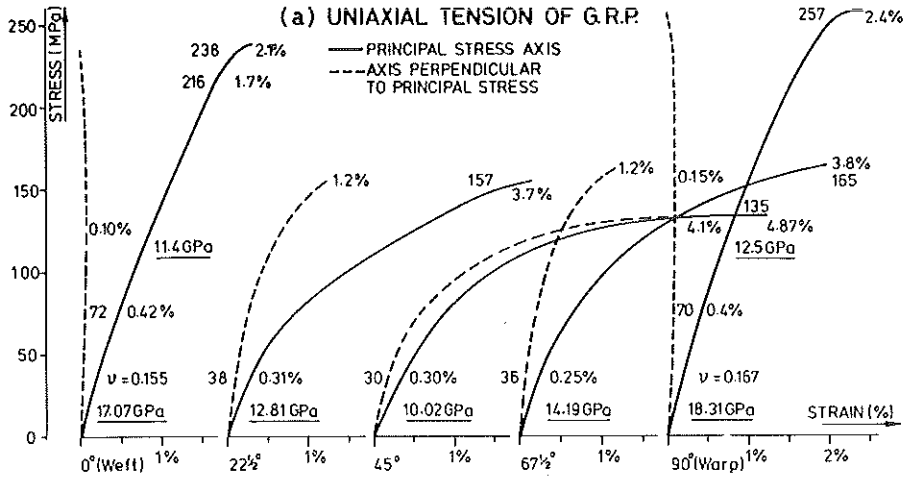

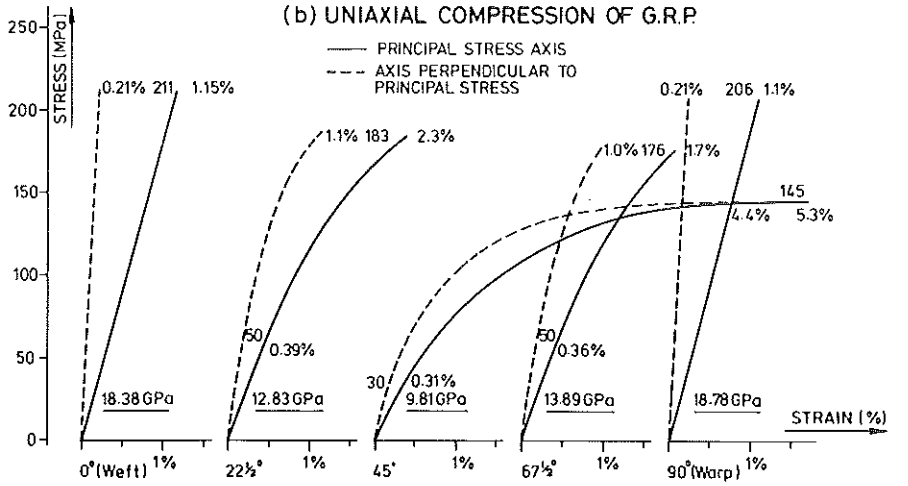

Fig 3 Monotonic stress/strain curves for uniaxial loading at various angles to the weft fibres. Adjacent to each curve are shown initial moduli (underlined), stress (MPa) and strain levels at 'knee' or 'yield', secondary moduli (underlined) if stress/strain curve remains linear above the 'knee', and failure stress (MPa) and strains

behaviour is reflected in a linear stress/strain curve. The failure plane could be of two types: a single shear plane as described by Levenetz (**36**) or a double shear or 'V' type mode. In compression, both the failure stresses and strains are less than in tension; no buckling of the specimen was apparent and the lower strengths can only be explained by the inability of the resin to transmit further interlaminar shear stress.

Off-axis loadings at $22\frac{1}{2}$, 45, and $67\frac{1}{2}$ degrees show a limit of stress strain proportionality for both tensile and compressive loading (see Fig. 3(b)). There is no distinct 'knee' as for the 0 and 90 degree axes, but instead there appears to be a true yield point above which, with increasing stress, flow progressively dominates. The yield stress decreased with increasing off-axis angle so that the 45 degree off-axis loading behaviour is dominated by a low yield and a low flow stress. Whatever the off-axis angle, tensile failure is along the fibre plane and fibres tend to pull out rather than fracture. The strain to failure also increased with increasing off-axis angle.

Fibre debonding and resin cracking are inherent with the 'knee' for the 0 and 90 degree loading cases, but the off-axis 'yield' does not appear to be accompanied by any direct signs of macro-damage until much higher strain levels, when a whitening of the resin is noted. Well above the tensile yield point signs of fibre debonding and resin cracking are also seen, both are aligned with the fibre direction, but the greater off-axis angles are dominated by resin whitening.

Equibiaxial loading ($\lambda = +1$)

Only one weave angle needs be tested for the equibiaxial case as the in-plane stress situation is not affected by direction (in-plane shear stresses are zero). With this in mind, only the tensile stress/strain behaviour along the two weave axes (0 and 90 degrees) has been studied (see Fig. 4(a)). The 'knee'' occurs along both axes, but the stress is slightly higher than if the stresses were applied separately. As a consequence the fibre-debonding and resin cracking along each axis accumulates at a slightly lower rate, but the combined extent of cracking is greater. Compared with the uniaxial stress state, the absence of in-plane shear stresses did not show any marked change in the stress/strain behaviour, apart from one factor. Under uniaxial loading the failure strain is greater for the warp (90 degrees) than for the weft (0 degrees) direction due to decrimping of the warp fibres, but under equi-biaxial loading the failure strain was found to be greater in the weft than the warp direction. Tension in the weft or transverse fibres would appear to stop the straightening of the warp fibres and so prevent any further strain component.

The combination of increased rectilinear cracking (fibre debonding and resin cracking) and induced interlaminar shear stresses through the high stress gradient between warp and weft fibres accelerates delamination and, hence, final fracture.

Equi-biaxial compression results in stress/strain linearity up to final failure, whatever the weave angle; the absence of any in-plane shear means that even

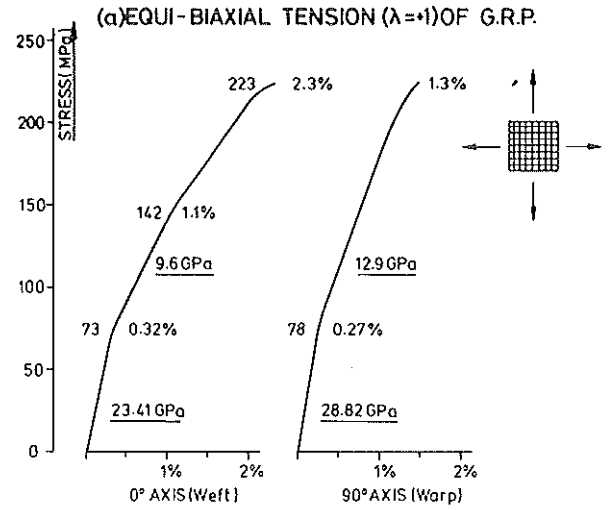

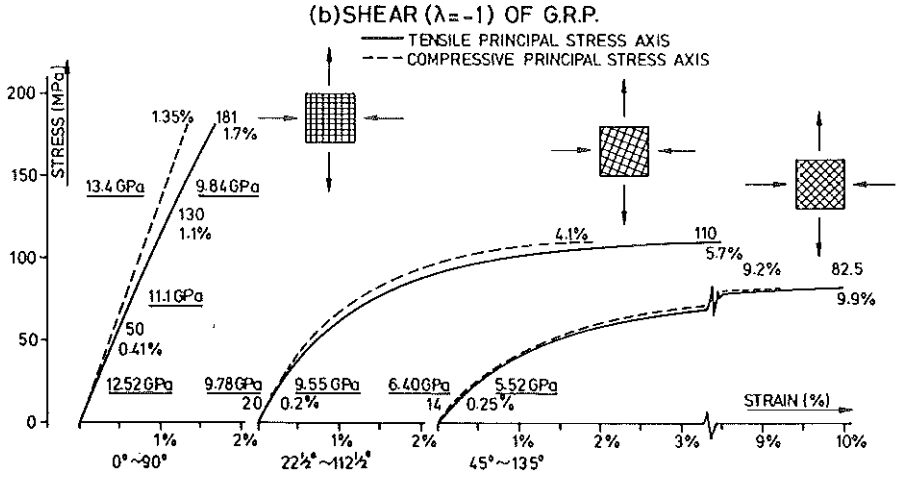

Fig 4 Monotonic stress/strain curves for biaxial loading at various angles to the fibres. Adjacent to each curve are shown initial moduli (underlined), stress (MPa) and strain levels at 'knee' or 'yield', secondary moduli (underlined) if stress/strain curve remains linear above the 'knee', and failure stress (MPa) and strains.

continued

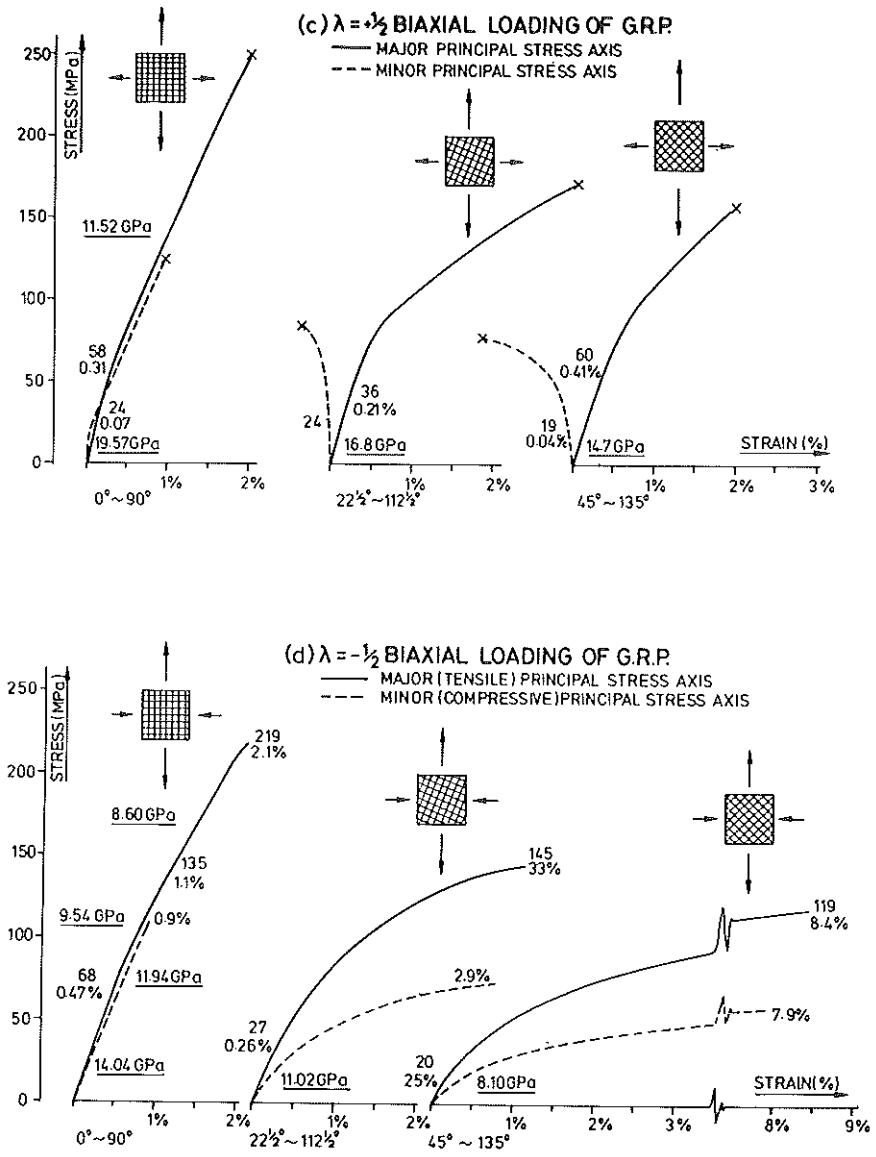

Fig 4 *continued* **The monotonic tension tests for $\lambda = +\frac{1}{2}$ resulted in premature failure of the loading arms, only the low and intermediate stress/strain behaviour is shown.** *NB.* **The fracture strength denoted here by (×) should be higher**

the 45 and 135 degree axes equibiaxial test shows no yield point. This highlights the fact that it is the in-plane shear which causes the yield under off-axis loading.

Shear loading ($\lambda = -1$)

The two extremes of in-plane biaxial stress are $\lambda = +1$ (equi-biaxial) and $\lambda = -1$ (shear) with the principal stress axes at 45 and 135 degrees to the weave axes. In the former case there are no in-plane shear stresses and in the latter case a state of pure in-plane shear exists with the maximum in-plane shear stress aligned with the fibres. The stress/strain curve for this extreme shear case is shown in Fig. 4(b). It results in a low failure stress with the stress/strain behaviour dominated by a low yield followed by considerable plastic flow with a shear strain at failure of 19 per cent.

Resin whitening is discernible at approximately 40 MPa (1 per cent strain) which gradually increases in intensity with increasing stress and at 75 MPa (90 per cent of ultimate stress) long white tracts can be seen running diagonally across the specimen; that is, aligned with the fibres and the direction of maximum shear. Prior to failure there was little sign of delamination and no evidence of rectilinear cracking. The plane of failure coincides with the plane of maximum shear and runs parallel with the fibres (see Fig. 5).

If $\lambda = -1$ and the principal stress axes are coincident with the weave axes there are no in-plane shear stresses aligned with the fibres. The stress/strain behaviour is as though the tensile and compressive components of stress were applied separately (see Fig. 4(b)). There are no signs of in-plane shear deformation and the final fracture mode is aligned with the fibres rather than the direction of maximum shear (see Fig. 5).

For $\lambda = -1$ and the principal stress directions at $22\frac{1}{2}$ and $112\frac{1}{2}$ degrees to the weave a condition exists where both normal stress and shear stresses act on the

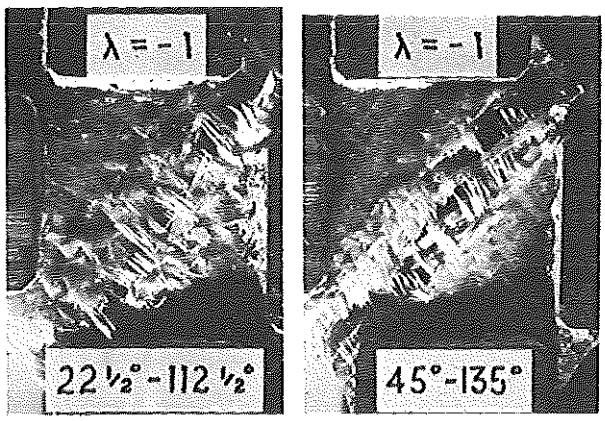

Fig 5 Monotonic failure under shear loading with principal stresses at $22\frac{1}{2}$ and $112\frac{1}{2}$ degrees, and 45 and 135 degrees to the fibres

fibre plane; i.e., this case is essentially similar to the uniaxial $22\frac{1}{2}$ degree off-axis loading situation, except for the difference in the ratio of normal to shear stress on the fibre plane. The stress/strain curve and appearance of failure are shown in Figs 4(b) and 5, respectively.

Biaxial loading with $\lambda = +\frac{1}{2}$ and $\lambda = -\frac{1}{2}$

The two biaxial loading conditions of $\lambda = +\frac{1}{2}$ and $\lambda = -\frac{1}{2}$ were tested to help establish a failure ellipse for the grp material. All the $\lambda = +\frac{1}{2}$ monotonic tests resulted in premature failure of the loading arms, but it was possible to ascertain the low and mid stress behaviour.

For the $\lambda = +\frac{1}{2}$, 0 and 90 degree case a distinct 'knee' is seen on both the major and minor axes (Fig. 4(c)), the former appears at a stress level of 58 MPa, and corresponds with the 'knee' seen in the uniaxial and shear loading cases. The minor axis 'knee', on the other hand, is at a stress level of only 24 MPa and 0.07 per cent strain, and is accompanied by the usual rectilinear cracking. The appearance of the tensile 'knee' is neither stress nor strain dependent, in fact, from the $\lambda = +\frac{1}{2}$ test the appearance of a 'knee' on the *minor* stress axis at such a low stress and strain points towards the tensile 'knee' being dependent on total strain energy.

Off-axis loading and $\lambda = +\frac{1}{2}$ not only results in marked shear deformation, but the Poisson effect between the principal stress axes increases as the off-axis angle is increased so that the minor stress axis shows a negative strain with respect to the minor principal stress (see Fig. 4(c)).

The $\lambda = -\frac{1}{2}$ load ratio shows stress/strain behaviour and fracture strengths between the uniaxial and shear cases (see Fig. 4(d)). Fracture for all fibre angles is aligned with the fibres.

Uniaxial and biaxial fatigue failure

Three series of uniaxial fatigue tests were completed to establish the effect of weave direction on fatigue strength. Then nine series of biaxial fatigue tests were made; a tenth, $\lambda = +\frac{1}{2}$ with 45 and 135 degree fibre axes, proved unsuccessful due to premature failure of the loading arms. The equibiaxial case ($\lambda = +1$) was made for 0 and 90 degree axes only. S–N curves are presented in Fig. 6 for all twelve series.

Loading with 0 and 90 degree principal axes

When the directions of principal stress coincide with the fibre axes, the nature of progressive fatigue damage shows the same pattern of behaviour whatever the ratio of loading. Fatigue is a bulk process and appears through cracking in the resin-rich areas between roving groups and the debonding of fibres transverse to the principal stress direction(s). The appearance and growth of resin cracking and fibre debonding is generally consistent with, and perpendicular

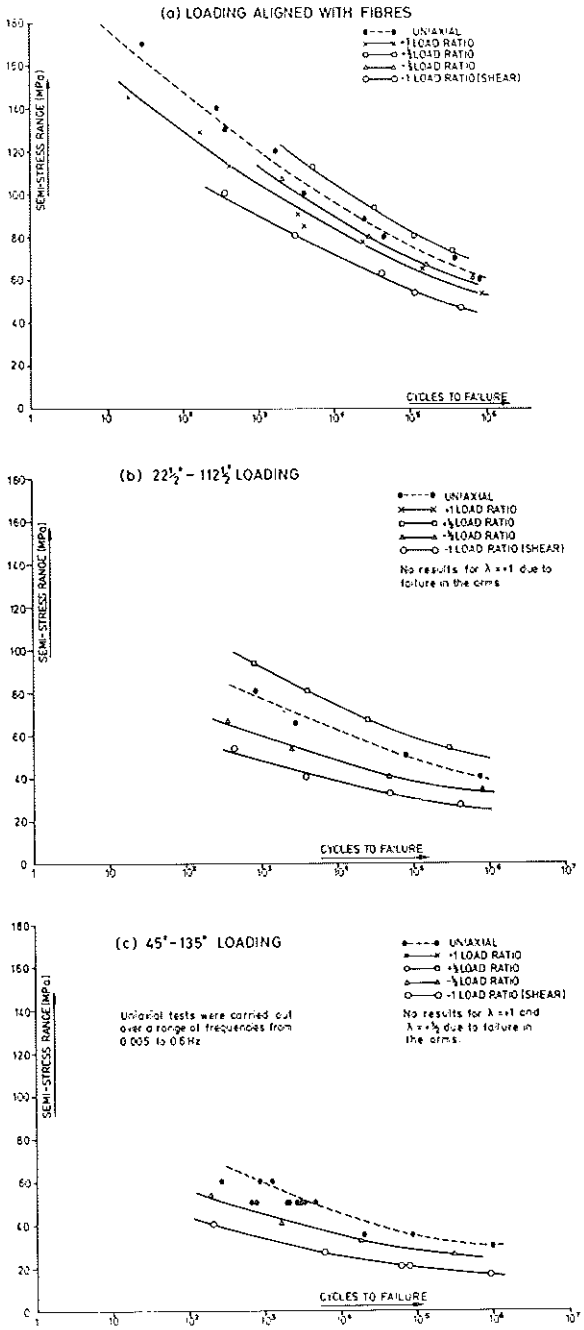

Fig 6 Principal semi-stress range versus fatigue life for loading at various angles to the fibres

to, the direction of the applied principal tensile stress(es), and the two phenomena will be described collectively as rectilinear cracking.

Cracks, whether initiating in resin rich areas or through debonding of transverse fibres, propagate across the particular area of initiation until running into one of four types of interface.

(1) Resin rich area to transverse fibre group.
(2) Transverse fibre group to resin rich area.
(3) Resin rich area to fibre group aligned with the principal stress.
(4) Transverse fibre group to aligned fibre groups.

Interfaces (1) and (2) tend not to interfere with the direction of crack propagation, though when the straight resin crack propagates into a transverse fibre group it may wander as it picks the weakest line. Interfaces (3) and (4), on the other hand, will tend to stop crack advance in a direction perpendicular to the principal stress. The strength and stiffness of the aligned rovings resist crack advance and the resultant stress concentration causes breakdown of the weak interface area, so promoting delamination. A number of cracks will propagate independently and cause separate areas of interface breakdown which subsequently join together as delamination. Cracking, fibre debonding, interface behaviour, and delamination are illustrated in Fig. 7.

In the high stress/low cycle positive load ratio tests delamination was often only localised, but for the high cycle tests, in particular those of negative load ratio, the surface laminates became entirely detached before final specimen collapse.

All the results and discussion appertain to zero mean stress fatigue, but observations of rectilinear cracking and delamination for two uniaxial fatigue tests with extremes of mean stress, zero-tension, and zero-compression loading, have helped in the understanding of the nature of progressive damage and the cyclic stress/strain behaviour. The semi-stress range for both these tests was

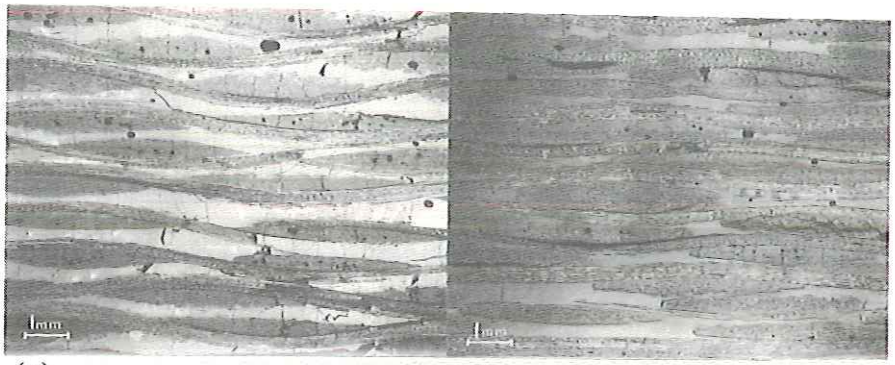

Fig 7 Appearance of macroscopic damage showing (a) rectilinear cracking and delamination under normal loading, and (b) fibre/matrix degradation and delamination under shear coincident with the fibre plane

75 MPa which gives a zero mean stress life of 10^5 cycles. Zero-tension loading reduced the life to 4247 cycles, and zero-compression even further to 2067 cycles. For the tensile loading case the characteristic 3-phase accumulation of cyclic strain range (Fig. 8(a) shows, for example, the accumulation of strain under equibiaxial cyclic loading) was evident, and sources of delamination were apparent after approximately 10 per cent life. This early delamination

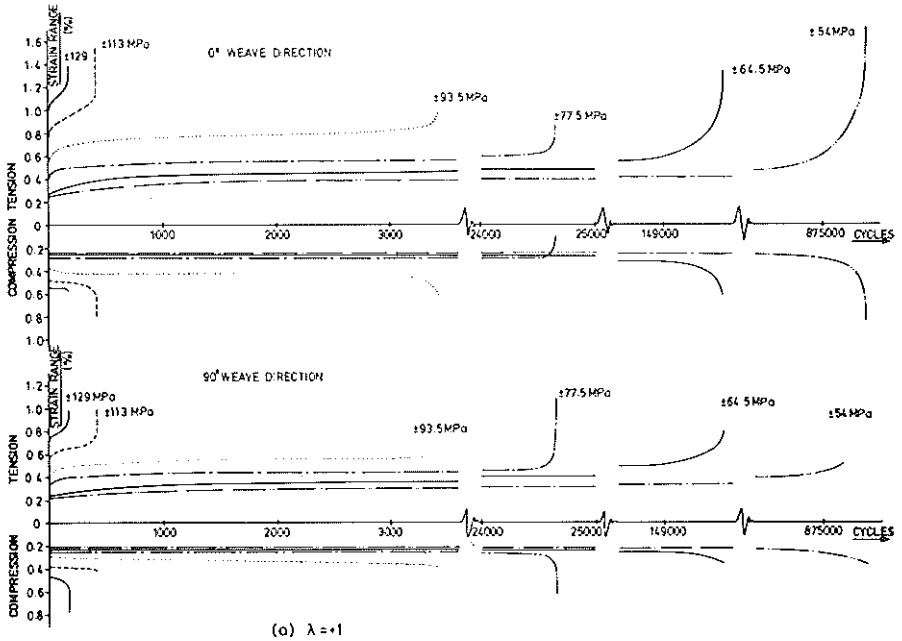

(a) λ = +1

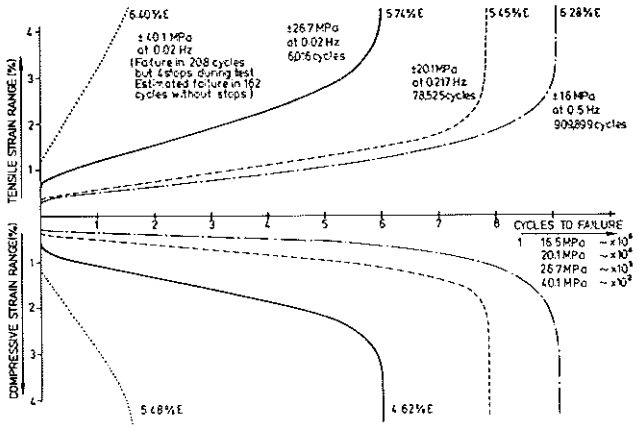

(b) λ = −1, 45°–135° LOADING

Fig 8 Three-phase accumulation of strain range; only the extreme cases of biaxial loading are presented

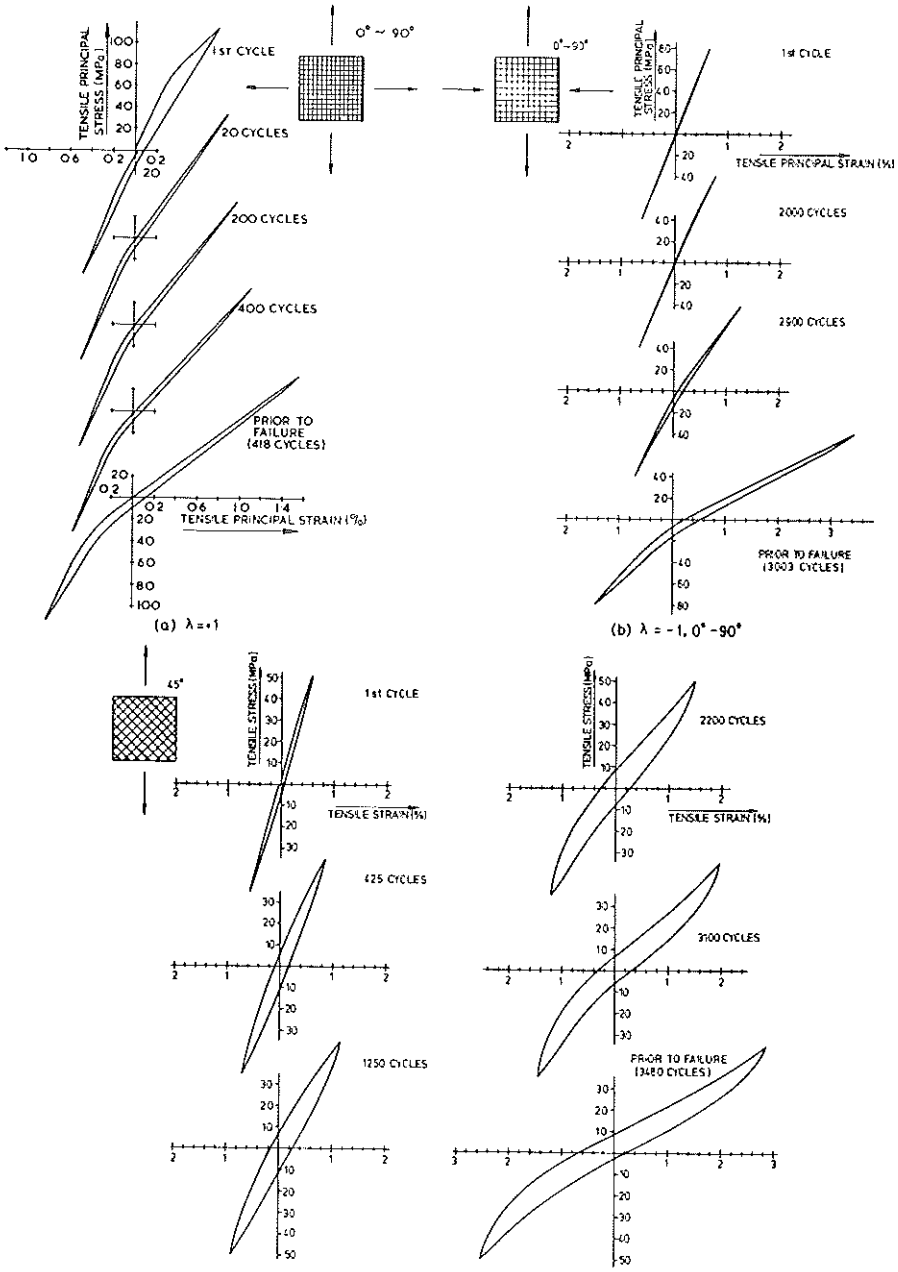
0° ~ 90°
1st CYCLE
20 CYCLES
200 CYCLES
400 CYCLES
PRIOR TO FAILURE (418 CYCLES)
TENSILE PRINCIPAL STRESS (MPa)
TENSILE PRINCIPAL STRAIN (%)
(a) λ = +1
0°~90°
1st CYCLE
2000 CYCLES
2500 CYCLES
PRIOR TO FAILURE (3003 CYCLES)
(b) λ = -1, 0° -90°
45°
1st CYCLE
425 CYCLES
1250 CYCLES
2200 CYCLES
3100 CYCLES
PRIOR TO FAILURE (3480 CYCLES)
TENSILE STRESS (MPa)
TENSILE STRAIN (%)
(c) λ = 0, UNIAXIAL 45°

Fig 9

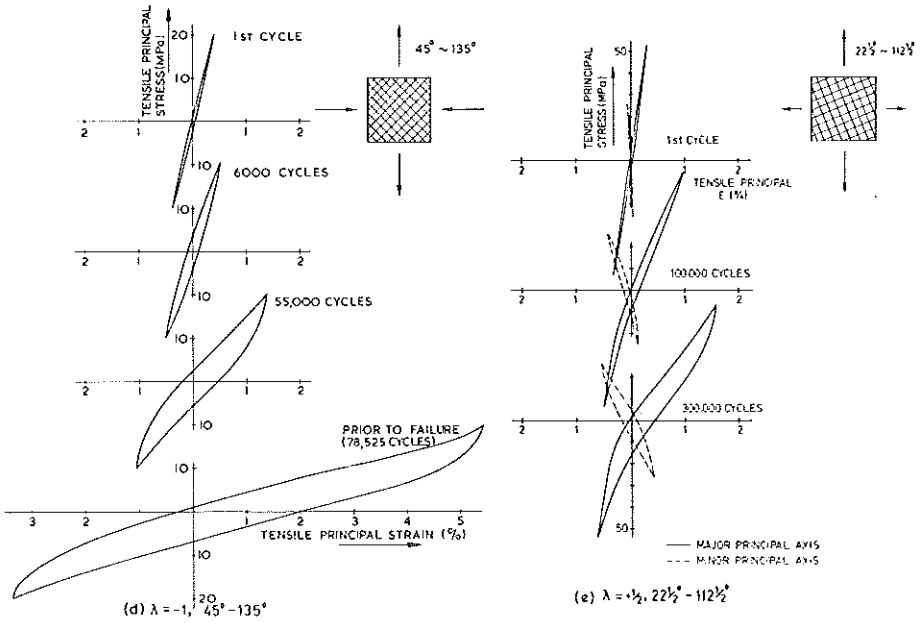

Fig 9 Progressive stress/strain loops of major principal (i.e., weft) axis for five cases of biaxial loading

dominated failure, and at 95 per cent life the advanced stages of delamination were causing an apparent buckling of the specimen at zero stress. Failure was of the 'brush' type mode characteristic of static tensile failure. Compressive fatigue loading showed no signs of transverse cracking and, even prior to failure, little sign of delamination. There was no discernible drop in modulus and the fracture mode was identical with that of the zero mean stress fatigue tests.

Though results from the two tests cannot serve any purpose in quantifying mean stress effects, they show the following.

(1) Delamination is a consequence of resin cracking and transverse fibre debonding which, in turn, are consequences of tensile loading.
(2) Delamination is not initiated by compressive loading; however, for zero mean stress loading, it is often first noticed in the compressive half cycle due to macro-buckling of the delaminated roving groups.

The extent to which the tensile and compressive halves of the loading cycle contribute towards damage and failure is not understood. For fatigue loading along the fibre axes, any non-linearity or 'knee' in the stress/strain curve occurs only on the first tensile-loading cycle (assuming constant maximum stress); it disappears on unloading and upon subsequent re-loading (see Fig. 9(a)) so that

an immediate drop in material modulus results. The 'knee' and, hence, the subsequent drop in modulus is caused by rectilinear cracking and the drop in modulus may, therefore, be expected to be a measure of the permanent damage. But fatigue damage during the compressive cycle does not cause as significant a change in modulus and yet, from the test carried out under zero-compression loading, the compressive half cycle would seem the most damaging. Much of the visible damage in the zero mean stress fatigue of grp occurs in the tensile half cycle, but the final failure of all fatigue tests was in compression.

The effect of load ratio (λ) on fatigue strength appears to be related to the extent of resin cracking, fibre debonding, and delamination induced on each complete loading cycle. For uniaxial loading ($\lambda = 0$) the rectilinear cracking will be confined to one direction, i.e., perpendicular to the principal stress direction. For $\lambda = +1$ rectilinear cracking was along both fibre axes, thus increasing the possible sites of delamination. Damage was seen to progress in a similar way to uniaxial loading, but at a greater rate.

For negative load ratios, i.e., where the in-plane shear stress is greater than $\sigma/2$ (where σ is the maximum principal stress) it would be expected that the mechanism of failure could change towards some form of shearing mode. This was not the case, and even for $\lambda = -1$ there was no evidence of in-plane shear deformation (Fig. 10). Although one effect of a negative load ratio is to reduce the effective composite stiffness (the Poisson strains work in the same sense as the principal strains), the real consequence is a more rapid accumulation of delamination through the simultaneous action of tensile and compressive forces. Delamination will be further aggravated because sources will appear through rectilinear cracking along both fibre axes as the sign of loading reverses for each half cycle.

The intermediate ratio of $\lambda = -\frac{1}{2}$ shows a behaviour somewhat between that for $\lambda = 0$ and $\lambda = -1$. The intermediate ratio of $\lambda = +\frac{1}{2}$, on the other hand, results in a greater fatigue strength than for either $\lambda = 0$ or $\lambda = +1$. If, for cyclic stresses along the fibre axes, the process of fatigue can be recognised solely as the accumulation of rectilinear cracking and delamination, it would be expected that the maximum fatigue strength would occur between $\lambda = 0$ and $\lambda = +1$; it may not necessarily be for the plane strain state ($\lambda = 0.16$) because, under load control, the state of strain can progressively change.

For loading along the fibre axes the cyclic stress/strain behaviour is asymmetric about the zero mean strain (Fig. 9(a) and (b)) and the shape of the stress/strain loop is basically similar for all load ratios. The loop is characterised by low hysteresis and a lower effective modulus in tension than compression. The change in modulus from tension to compression is shifted towards the compressive half cycle and, because of the low hysteresis, this change is seen on both loading and unloading. The resultant loop has a distinct 'crooked' appearance which becomes more so as the tensile modulus decreases at a greater rate than its compressive counterpart.

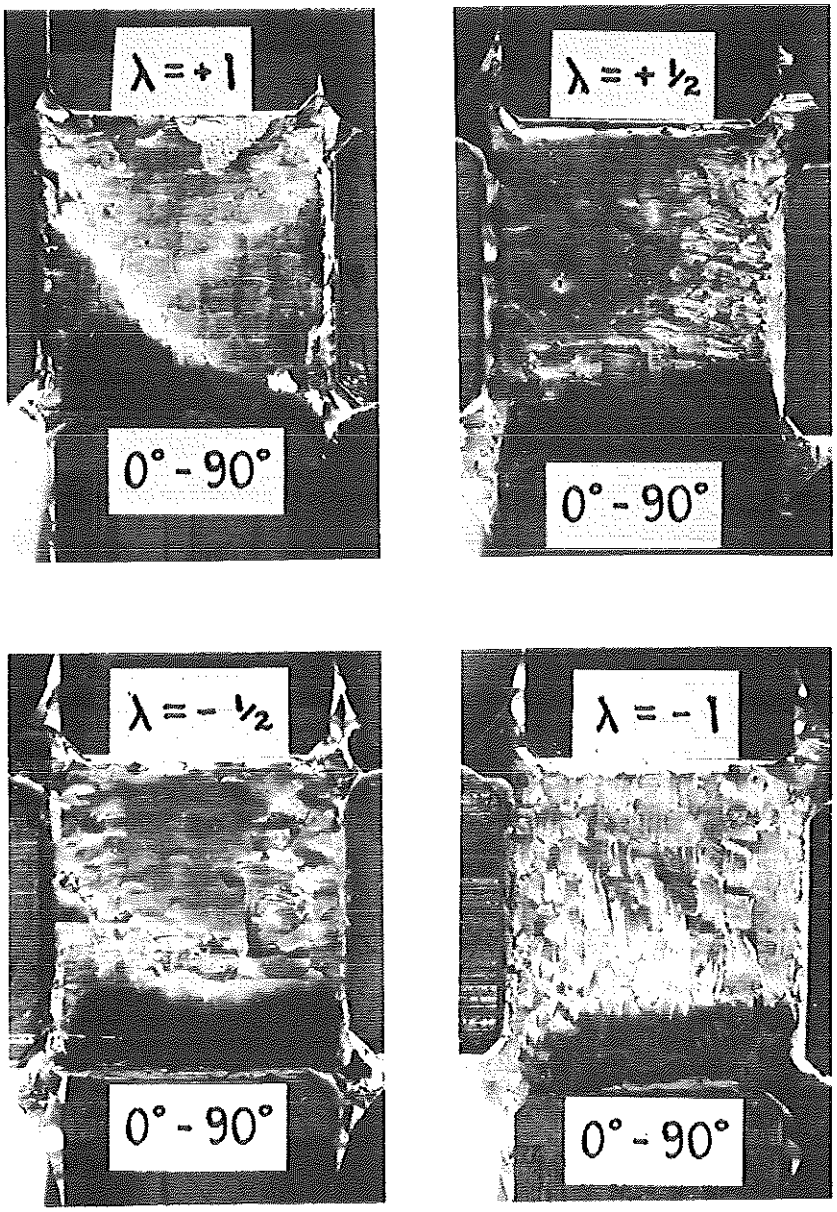

Fig 10 Fatigue failure modes, 0 and 90 degrees loading

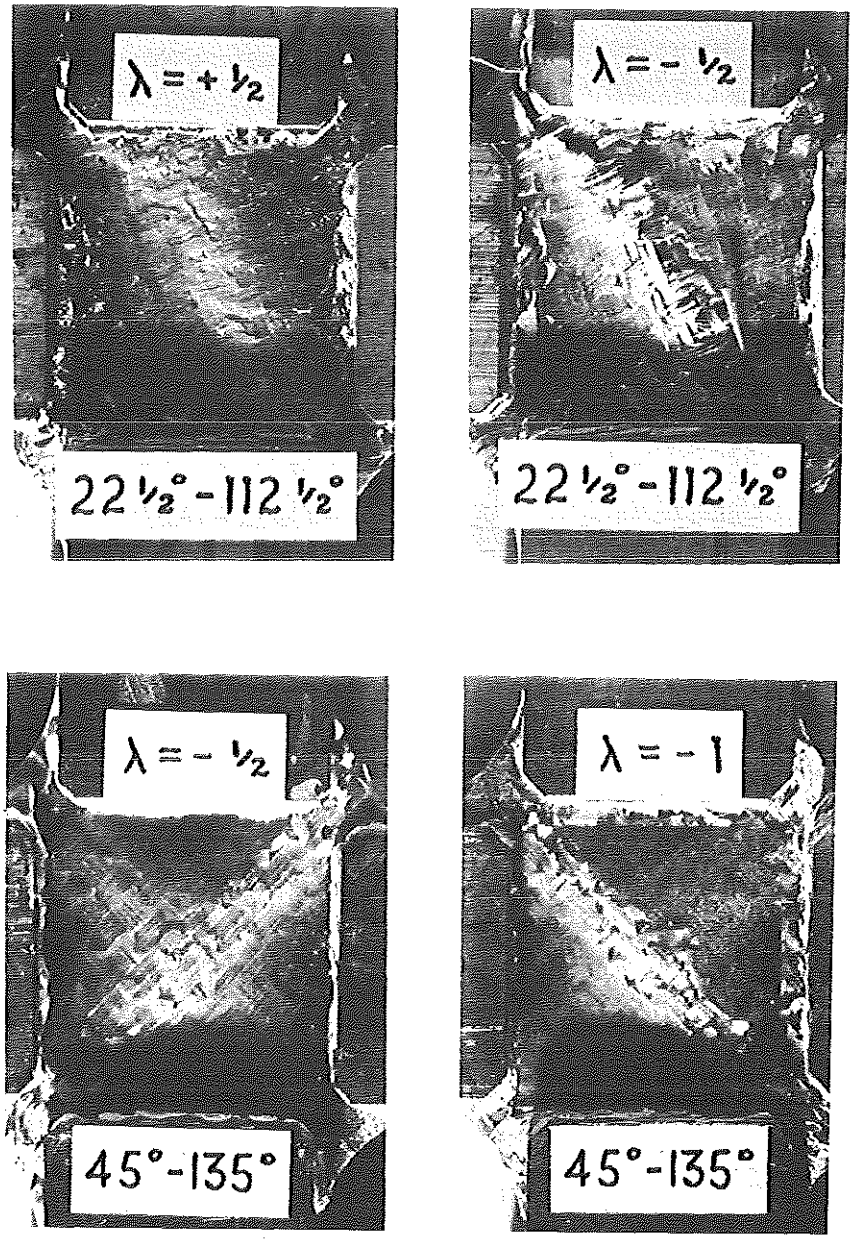

Fig 11 Fatigue failure modes, for $22\frac{1}{2}$ and $112\frac{1}{2}$ degrees loading and for 45 and 135 degrees loading

Loading with 45 and 135 degree principal axes

In contrast to 0 and 90 degree loading the cyclic stress/strain behaviour for 45 and 135 degree off-axis loading shows a marked variation with load ratio and, consequently, a greater change in fatigue strength with λ.

For a perfect state of equi-biaxial stress ($\lambda = +1$) the direction of the principal load axes should be immaterial and symmetrically disposed 45 and 135 degree axes would be expected to show identical cyclic stress/strain behaviour and strengths as for the 0 and 90 degree axes. Considerable effort was made to prove this experimentally, but the tests were unsuccessful due to premature fracture of the loading arms; on consideration of the difference between the equi-biaxial strength and the 45 degree uniaxial strength (223 MPa compared with 134 MPa, respectively) this premature failure is understandablee. Even so, the early life cyclic stress/strain behaviour for equibiaxial loading and 45 and 135 degree loading axes was similar to the 0 and 90 degree case, and resin cracking and fibre debonding was in line with the fibres rather than the loading arms. The stress/strain 'loop' for low stress loading was linear, except for a small change in modulus on load reversal, and, as a consequence, there was no hysteresis.

In the $\lambda = -1$ loading case with 45 and 135 degree principal stress axes the fibres are subjected to pure shear and no in-plane normal stresses. Cyclic loading of this type is characterised by a 1st cycle stress/strain loop of high hysteresis and second and subsequent stress/strain loops becoming progressively more non-linear as fatigue progresses (see Fig. 9(d)). This stress/strain non-linearity, and its subsequent persistence with cyclic loading, indicates a true plastic yield of the material rather than a damage phenomenon as is the 0 and 90 degreee 'knee'. The 1st cycle stress/strain loop is symmetrical about zero strain (controlled stress limits) and the shape and extremes of the loops are the same for both principal stress axes. As in the 0 and 90 degree loading cases, the accumulation of strain range up to final failure is characterised by three phases (see Fig. 8(b)), and, though the rate of accumulation for $\lambda = -1$ and 45 and 135 degree axes is much higher in each phase, only in the tertiary phase is the strain range greater in tension than compression. The high rates of strain range accumulation result in failure shear strains of the order of 10 per cent, compared with axial strains of 3 per cent or less for $\lambda = -1$ and 0 and 90 degree principal stress axes.

The appearance of progressive damage and failure for $\lambda = -1$ and 45 and 135 degree principal stress axes are dominated by shear deformation of the polymer matrix and shear degradation of the fibre/matrix interface. There are no signs of rectilinear cracking perpendicular to the fibres or to the tensile principal stress direction, and progressive damage appears as whitening of the laminate in line with the fibres (also the direction of maximum in-plane shear). Under high stress levels whitening appears in the first cycle, but at low stresses may not be apparent during the early stress cycles, even though the yield point has been exceeded. As shown in Fig. 7, delamination follows the later stages of pro-

gressive fibre/matrix interface breakdown and, even though the fibres become severely debonded, there are no signs of fibre fracture until final specimen failure. In fact, a realistic point of failure is difficult to assess due to the composite gradually losing strength because of severe matrix degradation and the flow stress of the material decreasing to such an extent that the fibres fail through lack of support from the matrix. Damage accumulates uniformly over the whole specimen until in the tertiary stage one or other of the maximum shear planes shows a more rapid accumulation. This dominant plane becomes the fracture plane, as shown in Fig. 11.

Cyclic shear loading with 45 and 135 degree principal stress axes results in very different macro-deformation to loading with 0 and 90 degree principal stress axes. This is exemplified, not only from the physical appearance of progressive damage and final failure, but also through the cyclic stress/strain behaviour. Assessment of the cyclic stress/strain behaviour when the principal stress directions are coincident with the fibre axes shows the composite deformation to be split into three components.

(1) Elastic deformation of both fibres and matrix.
(2) Linear viscoelastic deformation of the matrix.
(3) Deformation due to permanent damage, that is through:
    (i) resin cracking;
    (ii) transverse fibre debonding;
    (iii) delamination.

Each of these components is linearly related to stress, and only one, the viscoelastic component, is strain-rate dependent. On the other hand, cyclic shear loading with 45 and 135 degreee principal stress axes results in macro-deformation which is split into five components.

(1) Elastic deformation of the fibres and matrix.
(2) Plastic deformation of the matrix.
(3) Deformation due to permanent damage, that is caused by:
    (i) shear degradation of the fibre/matrix interface;
    (ii) delamination.
(4) Anelastic deformation of the matrix.
(5) Linear and nonlinear viscoelastic deformation of the matrix.

(1) and part of (5) are linearly related to stress, but the extent of each of the other components of deformation is difficult to quantify as the anelastic and viscoelastic parts are both rate or time dependent and non-linear. The extent of the anelastic component for a cyclic stress level less than 50 per cent ultimate is seen in Fig. 12(a), which shows the stress/strain loops for the 1st cycle and after 90 per cent life under uniaxial 45 degree off-axis reversed loading (50 MPa).

A more pronounced example of the anelastic behaviour is seen in Fig. 12(b) which shows 1st, 2nd, and 3rd stress/strain loops for non-reversed sinusoidal

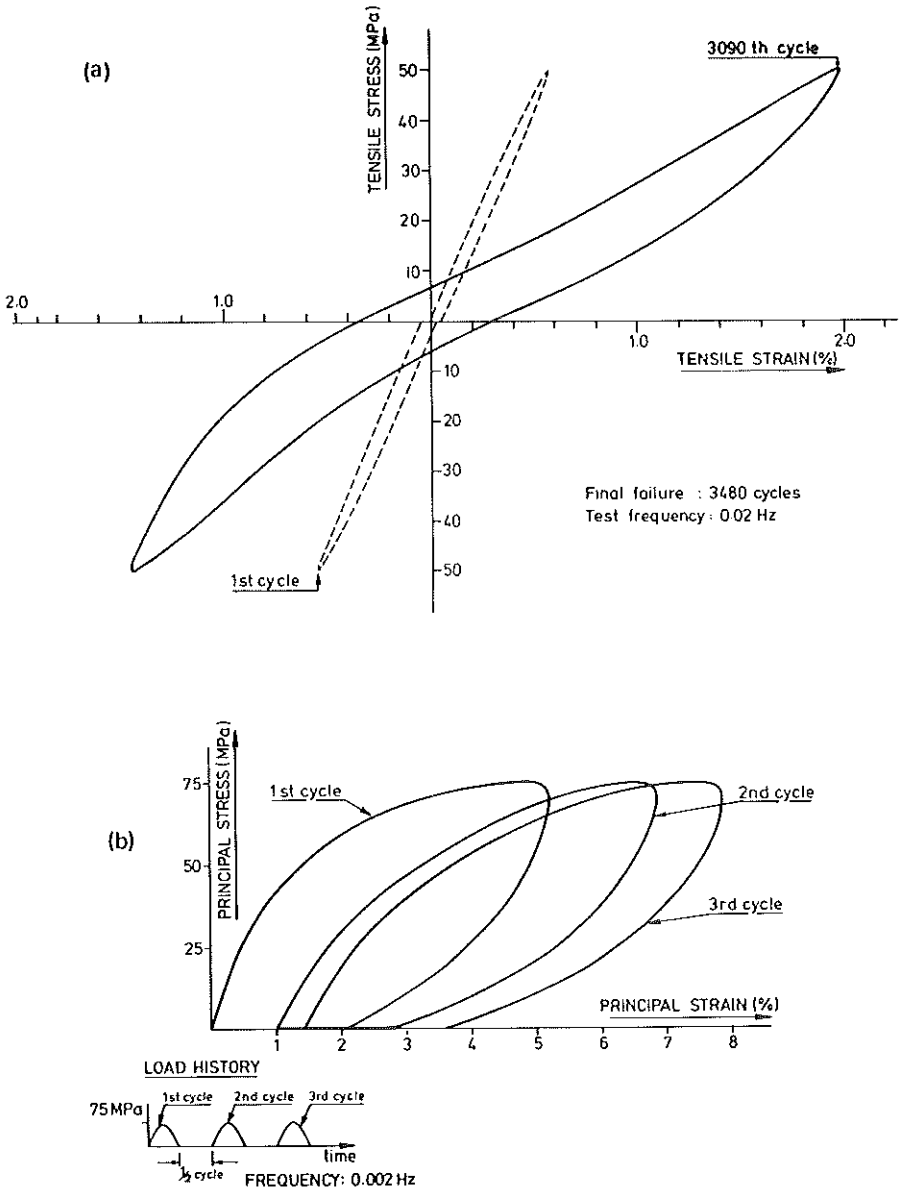

Fig 12 Stress/strain loops (a) for uniaxial 45 degree loading at 1st cycle and 3090 cycles, and (b) showing pronounced anelastic behaviour under non-reversed shear loading with 45 and 135 degree fibre axes

shear loading ($\lambda = -1$, 45 and 135 degree axes) made under a test frequency of 0.002 Hz and stress level of 75 MPa (90 per cent ultimate). After each half load cycle the load was held at zero for an equivalent half cycle (4.17 minutes). Rate or time dependent behaviour can be recognised from the following.

(1) A rounded extremity to the stress/strain loop at maximum stress.
(2) A non-linear decrease in strain with decreasing load.
(3) A 50 per cent recovery in the residual strain during 'hold' of the load at zero.

The accumulation of strain range with cycling is due to increased macro-damage, that is, breakdown of the fibre/matrix bond and increased plastic deformation (micro-damage) of the matrix.

In contrast, shear loading ($\lambda = -1$) with principal stress axes coincident with the fibre axes showed none of the above phenomena, and, of particular note, hold times of the load showed no signs of anelasticity, either at maximum or zero stress.

The intermediate load ratios of $\lambda = +\frac{1}{2}$, 0 (uniaxial) and $-\frac{1}{2}$ with 45 and 135 degree principal stress axes do not present clear-cut stress situations as do the equibiaxial and shear loading cases. The fibres are subjected to both in-plane shear stresses and in-plane normal stresses; the result is that the appearance of damage and the stress/strain behaviour are of mixed character. $\lambda = +\frac{1}{2}$ showed substantial rectilinear cracking aligned with the fibre axes and, to a lesser degree, matrix whitening and matrix/fibre interface degradation. 1st cycle stress/strain non-linearities did not disappear with subsequent cycling, but the strain range showed a much greater increase in tension than compression. For uniaxial loading and $\lambda = -\frac{1}{2}$ the extent of matrix shear and matrix/fibre interface degradation was greater than rectilinear cracking, and this was borne out by the strain range increasing in compression as well as tension in the primary and secondary phases; if damage was due solely to crack opening, i.e., rectilinear cracking, it would show up only as an increase in *tensile* strain range.

No fatigue tests were completed successfully for $\lambda = +\frac{1}{2}$ due to premature failure of the loading arms, but for $\lambda = 0$ and $\lambda = -\frac{1}{2}$ the final failure plane was coincident with the fibre axes (see Fig. 11).

The total cyclic strain range prior to fatigue failure for $\lambda = 0, -\frac{1}{2}$, and -1 was of the order of 6–10 per cent, some twenty times greater than in the 1st cycle. This growth is due to a drop in the material's flow stress which is, in itself, a consequence of the degradation of the fibre/matrix interface and a breakdown in the capacity of the matrix to transfer shear from fibre to fibre. However, in the tertiary stage of fatigue, the effective stiffness of the material does not show the usual continuing drop with increasing load; on the contrary, the stiffness is seen to increase with increasing load (see Fig. 9(c) and (d)). Stress/strain behaviour of this nature has been noted in the cyclic torsion of clays (**37**) and steels (**38**). The former case is attributed to the gradual consolidation or re-arrangement of the clay particles, whereas, in the torsion of steels, it

occurred after excessive growth of a single fatigue crack in a tubular specimen. The advancing helical crack was no longer subject to pure shear at the advancing tip, but a restricted or tensile mode was becoming apparent. In grp the phenomenon can be explained by the excessive deformation resulting from fibre/matrix shear degradation causing fibres, which were initially subjected primarily to shear, to be distorted or pulled out of line to such an extent that they begin to bear more and more tensile load. Whatever the micromechanics of such stress/strain behaviour it would appear to be a phenomenon related to shear deformation.

Loading with 22½ and 112½ degree principal axes

Excessive or additional in-plane shear strain was not evident under monotonic loading with 22½ and 112½ degree axes, but under fatigue loading a progressive breakdown in the fibre/matrix interface, caused primarily by rectilinear cracking, appeared to induce higher in-plane shear strains than implied by the loading state. This was particularly evident for $\lambda = +1$ and $\lambda = +\frac{1}{2}$. In the former case, with the accumulation of rectilinear cracking, which was aligned with the fibre direction, there was a tendency for the fibres to align towards the loading axes with the eventuality that, as cracking progressed, the specimen centre section was forced to rotate about itself. The result was premature specimen failure, not in the arms themselves, but at the edge of the working section where there was a transition from uniaxial to equibiaxial loading and, consequently, a high shear strain gradient.

$\lambda = +\frac{1}{2}$ with 22½ and 112½ degree principal axes is initially a plane strain state (see Fig. 9(e)), but with accumulation of damage the major axis Poisson strain dominates the transverse or minor axis. The early stages of fatigue show a progressive stress/strain behaviour characteristic of rectilinear cracking, the stress/strain loop has little hysteresis, and the accumulation of strain range is greater in tension than compression; but signs of in-plane shear become apparent as cracking progresses and the stress/strain hysteresis builds up accordingly. Prior to failure the amount of in-plane shear deformation was excessive; it was not aligned with the maximum shear plane, but with the fibres, and caused the final fracture plane also to be along the fibres.

The appearance and accumulation of damage for $\lambda = 0$, $-\frac{1}{2}$, and -1 is characterised by a combination of rectilinear cracking and fibre/matrix interface shear. The two modes of damage occurred concurrently, but the latter did not appear to be brought on by the progressive cracking as in the $\lambda = +\frac{1}{2}$ case. Even though neither the principal stress directions nor the maximum shear planes were coincident with the fibre planes, it was the direction of the fibres which dictated the progress of damage and the final failure mode (see Fig. 11). In each case the first stress cycle/strain loop exhibited some hysteresis, the more negative the load ratio the greater the hysteresis. As with 45 and 135 degree

off-axis loading, the hysteresis remained in the second and subsequent cycles and built up as damage increased.

Progressive cyclic stress/strain behaviour

Both Broutman and Sahu (**10**) and Owen and Howe (**39**) have measured the density of cracking and fibre debonding in cyclic uniaxial loaded grp. The former tested a bi-directional non-woven composite and the latter a chopped-strand-mat composite. The increase in crack density with fatigue cycles showed the same three-phase pattern as the strain range increase for the grp. However, the increase in strain range under off-axis loading is not due solely to the accumulation of cracks, some part must be due to fibre/matrix shear degradation and delamination. Cracks running perpendicular to a principal stress will mainly affect the tensile strain range (due to crack opening) and cause only a little change (if any) in the compressive strain range, whereas fibre/matrix shear degradation will cause a change in the stress/strain characteristics whether the principal applied stress is tensile or compressive. In the initial and secondary phases of strain accumulation the compressive strain range for loading along the fibre axes increases only slightly, but in the tertiary phase a rapid increase in the compressive strain range as well as in the tensile strain range is witnessed. An obvious explanation for this exponential increase of strain range is the accumulation of delamination, but the beginning of the tertiary phase never appeared to coincide with the early signs of delamination. In fact, severe delamination could cause the surface-mounted gauges to record a drop in compressive strain range.

The long secondary phase of strain range accumulation shows a linear rate of increase with fatigue cycles, and is a minimum for any cyclic stress level. This pattern is similar to a creep curve for metals, e.g., (**40**), and Monkman and Grant (**41**) showed, for a large number of alloys, that there is a reasonable correlation between the secondary or minimum creep rate and the creep rupture life. They proposed the relationship

$$\log t_r + m' \log (mcr) = c$$

where

t_r = creep rupture life
mcr = minimum creep rate
m' and c are constants

A similar type of relationship was considered for the fatigue life of the test grp and the minimum or secondary strain range accumulation rate, i.e.

$$\log N_f = m' \log \dot{\varepsilon}_{min} + c$$

where

N_f = fatigue life

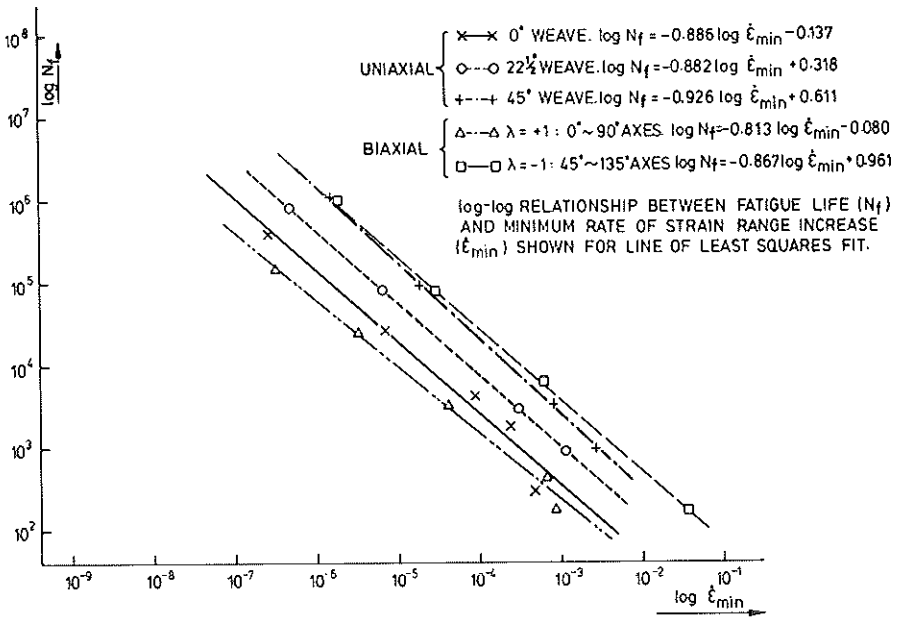

Fig 13 Fatigue life (N_f) versus minimum rate of strain range increase for uniaxial and biaxial loading

$\dot{\varepsilon}_{min}$ = minimum strain range accumulation rate

m' and c are constants

The relationship was applied to the sum of the tensile and compressive strain range accumulation rates for uniaxial loading and the extremes of biaxial loading $\lambda = +1$: 0 and 90 degree weave and $\lambda = -1$: 45 and 135 degree weave. The 'least square fit' lines are shown in Fig. 13. The straight line log–log relationship is shifted in the direction of increasing $\dot{\varepsilon}_{min}$ as the off-axis angle is increased, but the gradient, i.e., the constant m', is reasonably constant for all loading conditions.

The amount of test data backing the above analysis is small, so the relationship should be treated with some caution, but its use in predicting high cycle fatigue strengths or the probability of a fatigue limit ought to be considered. The fatigue strength is dependent on cyclic test frequency, particularly for off-axis loading and negative load ratios, and an optimum frequency for 45 degree uniaxial loading to minimize cyclic heating and cyclic creep is estimated to be of the order of 1 Hz for a stress level giving a life of 10^8 cycles, i.e., a test lasting longer than 3 years! If the constant m' is established from short life tests, then high cycle fatigue lives can be estimated once a test has progressed into the secondary phase.

Conclusions

Five distinct components of deformation have been recognized for the woven-roving glass-fibre composite in five loading states and three directions of weave axes.

(1) Elastic deformation of both fibres and matrix, rate independent and recoverable.
(2) Plastic deformation of the matrix (micro-damage), rate independent and non-recoverable.
(3) Deformation due to macro-damage, rate independent and non-recoverable:
    (i) rectilinear cracking (combined resin cracking and fibre/matrix debonding);
    (ii) shear degradation of the fibre/matrix interface;
    (iii) delamination.
(4) Anelastic deformation of the matrix, rate dependent and recoverable.
(5) Linear and non-linear viscoelastic deformation of the matrix, rate dependent and part recoverable.

Loading along the fibre axes results in the elastic component, the macro-damage components (i) and (iii) and a linear component of viscoelastic deformation. A pure shear stress along the fibre axes involves all the above components except the macro-damage (i). The general off-axis loading case results in all five components.

Macroscopic observation of damage and the interpretation of progressive cyclic stress/strain behaviour has shown that there are two distinct and very different mechanisms of failure.

(1) If the principal in-plane stresses are aligned with the fibre weave, then failure is a process of rectilinear cracking and delamination. The cyclic stress/strain behaviour is characterised by a 'knee' in the first quarter cycle of tensile loading which does not appear in the compressive half cycle or in subsequent tensile cycles, little or no hysteresis, and a cyclic build-up in strain range which is greater over the tensile half-cycle, so causing a crooked stress/strain loop. The failure mechanism does not alter with load ratio.
(2) For an in-plane shear stress concurrent with the fibres, failure is by a process of shear degradation at the fibre/matrix interface and delamination: the cyclic stress/strain behaviour is dominated by high hysteresis, and a true yield point is manifest for both tensile and compressive principal stress directions. The stress/strain behaviour is noticeably rate dependent. There are no signs of rectilinear cracking.

The failure mechanism for general off-axis loading shows a mixed behaviour with both rectilinear cracking and shear of the fibre/matrix interface. The extent of either mechanism depends on the off-axis angle and the load ratio.

A characteristic of all loading cases is that cracking, fibre/matrix interface degradation, and final fracture are always aligned with the fibres and not necessarily with the principal stress directions or the maximum shear plane.

Acknowledgements

The experimental programme was carried out at Cambridge University, UK, with the financial support of the Procurement Executive, Ministry of Defence. The authors wish to thank Mr P. R. Christopher, then of the Naval Construction Research Establishment, for his help and encouragement; and Mr R. J. Brand for assistance in carrying out the experiments.

References

(1) BROUTMAN, L. J. and KROCK, R. H. (1967) *Modern composite materials*, Addison-Wesley, New York.
(2) McCRUM, N. G. (1970) *A review of the science of fibre reinforced plastics*, HMSO, London.
(3) SENDECKYI, G. R. (1975) Mechanics of composite materials, *Composite materials* (Edited by BROUTMAN, L. J. and KROCK, R. H.), Academic Press, London, Vol. 2.
(4) DEW HUGHES, D. and WAY, J. L. (1973) Fatigue of fibre-reinforced plastics: A review, *Composites*, **4**, 167–173.
(5) OWEN, M. J. (1970) Fatigue, *Glass reinforced plastics* (Edited by PARKIN, B.), Iliffe, London.
(6) SALKIND, M. J. (1972) Fatigue of Composites, *Composite Materials: Testing and Design* (2nd Conf.), *ASTM STP 497*, ASTM, Philadelphia, PA, pp. 143–169.
(7) THROCKMORTON, P. E., HICKMAN, H. M., and BROWNE, N. F. (1963) Origin of stress failure in glass reinforced plastics, *Modern Plastics*, **40**, 140–150, 189–198.
(8) OWEN, M. J. and DUKES, R. J. (1967) Failure of glass reinforced plastics under single and repeated loading, *J. Strain Analysis*, **2**, 272–279.
(9) PLUMBRIDGE, W. J. (1972) Review: Fatigue-crack propagation in metallic and polymeric materials, *J. Mater. Sci.*, **7**, 939–962.
(10) BROUTMAN, L. J. and SAHU, S. (1969) Progressive damage of a glass reinforced plastic during fatigue, Proc. 24th Conf. SPI Reinforced Plastics Div., Sect. 11-D.
(11) CESSNA, L., LEVENS, J., and THOMSON, J. (1969) Flexural fatigue of glass reinforced thermoplastics, Proc. 24th Conf. SPI Reinforced Plastics Div., Sect. 1-C.
(12) AGARWAL, B. B. and DALLY, J. W. (1975) Prediction of low-cycle fatigue behaviour of GFRP: An experimental approach, *J. Mater. Sci.*, **10**, 193–199.
(13) PASCOE, K. J. and DE VILLIERS, J. W. R. (1967) Low-cycle fatigue of steels under biaxial straining, *J. Strain Analysis*, **2**, 117–126.
(14) PARSONS, M. W. and PASCOE, K. J. (1974) Low-cycle fatigue under biaxial stress, *Proc. Instn Mech. Engrs*, **188**, 657–671.
(15) EVANS, W. J. (1972) Deformation and failure under multi-axial stresses – A survey of laboratory techniques and experimental data, *NGTE Note NT 833*.
(16) LIDDLE, M. and MILLER, K. J. (1973) Multi-axial high-strain fatigue. Proc. 3rd Int. Conf. on Fracture, Munich, Pt. V523/A.
(17) ANDREWS, J. M. H. and TOPPER, T. H. (1973) A testing rig for cycling at high biaxial strains, *J. Strain Analysis*, **8**, 168–175.
(18) McCLAREN, S. W. and TERRY, E. L. (1963) Characteristics of aerospace materials subjected to biaxial static and fatigue loading conditions, ASME Paper 63-WA-315.
(19) FREUND, J. F. and SILVERGLEIT, M. (1966) Fatigue characteristics of GRP material, Proc. 21st SPI Reinforced Plastics Div., Sect. 17-B.
(20) IRWIN, L. H., DUNLOP, W. A., and COMPTON, P. V. (1974) Uniaxial, biaxial and fatigue properties of polyester fibre glass, *Composite Materials: Testing and Design* (3rd Conf.), *ASTM STP 546*, ASTM, Philadelphia, PA, pp. 395–418.
(21) BERT, C. W., MAYBERRY, B. L., and RAY, J. D. (1969) Behaviour of fibre-reinforced plastic laminates under biaxial loading. *Composite Materials: Testing and Design, ASTM STP 460*, ASTM, Philadelphia, PA, pp. 362–380.

(22) OWEN, M. J. and FOUND, M. S. (1972) Static and fatigue failure of glass reinforced polyester resins under complex stress conditions, *Faraday Special Discussions of the Chemical Society No. 2*, Chemical Society, London, pp. 77–89.
(23) OWEN, M. J. and GRIFFITHS, J. R. (1978) Evaluation of biaxial stress fatigue failure surfaces for a glass reinforced polyester resin under static and fatigue loading, *J. Mater. Sci.*, **13**, 1521–1537.
(24) OWEN, M. J. and RICE, D. J. (1982) Biaxial strength behaviour of glass-reinforced polyester resins, *Composite Materials: Testing and Design* (6th Conf.), *ASTM STP 787*, ASTM, Philadelphia, PA, pp. 124–144.
(25) JONES, E. R. (1968) Strength of glass filament reinforced plastics in biaxial loading, *26th Annual Tech. Conf.*, Society of Plastics Engineers, pp. 11–14.
(26) PROTOSOV, V. D. and KOPNOV, V. A. (1965) Study of the strength of glass reinforced plastics in the plane strain state, *Mekhanika Polimerov*, **1**, 39–44.
(27) PARSONS, M. W. and PASCOE, K. J. (1975) Development of a biaxial fatigue testing rig, *J. Strain Analysis*, **10**, 1–9.
(28) SMITH, E. W. and PASCOE, K. J. (1985) Practical strain extensometry for cruciform-shaped specimens – Part 2, *Strain*, 175–181.
(29) McGARRY, F. J. (1968) Crack propagation in fibre reinforced plastic composites, *Fundamental aspects of fibre-reinforced plastic composites* (Edited by SCHWARTZ, R. J. and SCHWARTZ, H. S.), Wiley, New York.
(30) ENDO, K. and WATANABE, M. (1971) Fatigue properties of fibrous reinforced plastics, *Proc. 14th Japan Congress on Materials Research*, Kyoto, pp. 120–123.
(31) FUJII, T., MIZUKAWA, K., and ZAKE, M. (1970) Fatigue model and non-destructive testing methods of fibre-glass reinforced plastics, *Proc. 13th Japan Congress on Materials Research*, pp. 197–199.
(32) McGARRY, F. J. and DESAI, M. B. (1959) Failure mechanisms in fibre glass reinforced plastics, Proc. 14th Conf. SPI Reinforced Plastics Div. Sect. 16-E.
(33) MEHAN, R. L. and MULLIN, J. V. (1971) Analysis of composite failure mechanisms using acoustic emissions, *J. Composite Materials*, **5**, 266–269.
(34) *Strength and stiffness through fibre orientation: Reinforced plastics design guide*, 3M Company.
(35) *Plastics for aerospace vehicles – Part 1: Reinforced Plastics* (1971) MIL-HDB-17A, Department of Defence, Washington, DC, 1971.
(36) LEVENETZ, B. (1964) Compressive applications of large diameter fibre reinforced plastics, Proc. 19th Conf. SPI Reinforced Plastics Div., Sect. 14-D.
(37) TAYLOR, P. L. and BACCHUS, D. R. (1969) Dynamic cyclic strain tests on a clay, *Proc. 7th Int. Conf. Soil Mechanics*, Mexico, Vol. 1, pp. 401–409.
(38) BROWN, M. W. *Private Communication*.
(39) OWEN, M. J. and HOWE, R. J. (1972) The accumulation of damage in a glass reinforced plastic under tensile and fatigue loading, *J. Phys D: Appl. Phys*, **5**, 1637–1649.
(40) GAROFALO, F. (1965) *Fundamentals of creep and creep-rupture in metals*, Macmillan, New York.
(41) MONKMAN, F. C. and GRANT, N. J. (1956) An empirical relationship between rupture life and minimum creep rate in creep-rupture tests, *Proc. ASTM*, **56**, 593–620.